

Published in final edited form as:

*Brain Behav Immun.* 2014 January ; 35: . doi:10.1016/j.bbi.2013.07.175.

## Dysregulation in Myelination Mediated by Persistent Neuroinflammation: Possible Mechanisms in Chemotherapy-related Cognitive Impairment

Teresita L. Briones<sup>1,\*</sup> and Julie Woods<sup>2</sup>

<sup>1</sup>Department of Adult Health, Wayne State University, Detroit, MI 48202

<sup>2</sup>Department of Biobehavioral Health Science, University of Illinois at Chicago, Chicago, IL 60612

### Abstract

Cognitive impairment is commonly reported as a consequence of chemotherapy and can have considerable impact on everyday life on cancer patients. Thus, it is imperative to have a clear understanding of this phenomenon and the underlying mechanism involved. In the present study we examined the role of neuroinflammation and myelination in chemotherapy-related cognitive impairment. Female Sprague-Dawley rats (12-months old) were used in the study (total n=52, 13rats/group). Rats were randomly assigned to either the chemotherapy or saline control group. The drug combination of cyclophosphamide, methotrexate, and 5-fluorouracil (CMF) was given i.p. once a week for 4 weeks. Rats in the control group received normal saline of equal volume. Animals from each group were further randomized to receive either: cyclooxygenase (COX-2) inhibitor, NS-393, to block the inflammatory response or vehicle. NS-398 was given at 10 mg/Kg i.p. and equal volume of saline (vehicle) was injected i.p. as vehicle. Both NS-398 and vehicle were injected one hour after the first CMF dose and then given daily for 28 days then rats were tested in the Y maze. Our data showed that: (1) CMF led to the increase in the levels of inflammatory mediators IL-1 $\beta$ , TNF- $\alpha$ , and COX-2 while levels of the anti-inflammatory cytokine IL-10 decreased; (2) cognitive impairment and neuroinflammation resulting from CMF persisted 4 weeks after the treatment ended; and (3) administration of NS-398 attenuated CMF-induced neuroinflammation and effects on myelin and cognitive impairment. These findings suggest the involvement of neuroinflammation in CMF-induced changes in myelin and myelination, and cognitive impairment.

---

Cognitive impairment is commonly reported as a consequence of chemotherapy in patients with cancer [reviewed in (Hodgson et al., 2013; Janelsins et al., 2011)]. The cognitive deficits reported are impairments in memory, attention, clarity of thought, executive functioning, and speed of information processing (Ahles and Saykin, 2002; Janelsins et al., 2010; Nelson et al., 2007). The impact of chemotherapy-related cognitive impairment on everyday life is considerable, with patients experiencing difficulty undertaking and completing simple tasks including paying the bills and preparing meals (Boykoff et al.,

---

© 2013 Elsevier Inc. All rights reserved.

\*Corresponding Author: Teresita L. Briones, Ph.D., Associate Professor, Department of Adult Health, Wayne State University, 5557 Cass Ave., Cohn Bldg, Rm 344, Detroit, MI 48202, USA, Telephone: (313) 577-4143, Fax: (313) 577-4188, tbriones@wayne.edu.

Conflict of Interest

The authors have no conflict of interest to declare.

**Publisher's Disclaimer:** This is a PDF file of an unedited manuscript that has been accepted for publication. As a service to our customers we are providing this early version of the manuscript. The manuscript will undergo copyediting, typesetting, and review of the resulting proof before it is published in its final citable form. Please note that during the production process errors may be discovered which could affect the content, and all legal disclaimers that apply to the journal pertain.

2009; Reid-Arndt, 2009). Moreover, individuals with chemotherapy-related cognitive impairment sometimes experience difficulty performing necessary work-related responsibilities (Castellon and Ganz, 2009; Reid-Arndt, 2009). Based on these reported complaints, it is clear that chemotherapy-related cognitive impairment can have a significant impact on personal, occupational, and social functioning that in turn can contribute to decreased quality of life.

Chemotherapy-related cognitive impairment will be a significant health care concern in the future because it is estimated that by year 2020, there will be approximately 70 million cancer survivors worldwide (Weiss, 2008). Estimates of the prevalence of chemotherapy-related cognitive impairment is from 16% to 85% (Correa and Ahles, 2007), a range too wide to convince those outside the patient population of the reality of cognitive impairments found in cancer patients undergoing or having completed chemotherapy. Despite ongoing research on chemotherapy-related cognitive impairment, an understanding of the underlying mechanisms of this phenomenon is still lacking. One of the proposed mechanisms consistently shown to be present in patients who received chemotherapy is damage to the brain white matter microstructure. Neuroimaging studies show altered white matter activation patterns in brain areas involved in cognitive functioning after standard dose chemotherapy (de Ruitner et al., 2011; Kesler et al., 2009; Silverman et al., 2007). Other studies using voxel-based morphometry also report reductions in white matter and to some extent gray matter in the prefrontal cortex and corpus callosum within one year after cessation of standard dosages of chemotherapy compared to cancer patients not receiving chemotherapy (Inagaki et al., 2007; McDonald et al., 2010). Studies using diffusion tensor imaging also show lower fractional anisotropy and increased diffusivity in the genu region of the corpus callosum, as well as in the frontal and temporal white matter areas two years after standard dose chemotherapy when compared to cancer patients that did not receive the treatment and age matched healthy subjects (Deprez et al., 2011). Also, functional magnetic resonance imaging studies show altered activation patterns in the posterior parietal cortex during memory encoding and executive functioning tasks in breast cancer survivors that received chemotherapy years earlier when compared to those that did not receive the treatment (Koppelmans et al., 2011; Koppelmans et al., 2012).

White matter abnormalities associated with chemotherapy are most likely due to the direct and/or indirect neurotoxicity effects of the drugs (Weiss, 2008). Generally, the blood-brain barrier is believed to prevent cytotoxic agents from entering the brain. However, there are reports that demonstrate some agents such as 5-fluorouracil can cross the blood-brain barrier mainly by diffusion (Sakane et al., 1999). Several preclinical studies also show that methotrexate and cyclophosphamide when administered systemically can disrupt cell division in certain brain regions critical for learning and memory (Briones et al., 2011; Seigers et al., 2008; Seigers et al., 2010a). Reports on mice show that 5-fluorouracil can damage myelin-forming oligodendrocytes and their precursor cells (Dietrich et al., 2006; Han et al., 2008). These reports point to the vulnerability of oligodendrocytes to the toxic effects of chemotherapeutic agents as a possible reason for the white matter abnormalities seen in imaging studies. However, the mechanism that mediates the toxic effects of chemotherapy on oligodendrocytes remains unclear.

Neuroinflammation begins as a host defense mechanism associated with neutralization of an insult and restoration of normal structure and function (Finnie, 2013). On the other hand, if neuroinflammation is not regulated, it can result in a self-propagating and deleterious process (Block and Hong, 2005). Microglial cells are considered to be the resident immune system of the brain and initiate the neuroinflammatory process as a reaction to various insults (Woodcock and Morganti-Kossmann, 2013) including chemical insults, induced by chemotherapy. Persistent neuroinflammation results in chronically activated microglia and

release of inflammatory mediators such as tumor necrosis factor- $\alpha$  (TNF- $\alpha$ ) and interleukin1-beta (IL1- $\beta$ ) that may lead to neuronal and glial cell damage. In the present study we examined the role of neuroinflammation and myelination in chemotherapy-related cognitive impairment.

## Methods

### Animal Model

Female Sprague-Dawley rats (12-months old) obtained from Harlan Laboratories (Madison, Wisconsin) were housed in pairs in a pathogen-free vivarium under controlled condition (temperature  $22 \pm 1^\circ\text{C}$  and humidity  $70 \pm 5\%$ ) and a 14:10 hour light:dark cycle was maintained. All animals were housed in the same room so that temperature, humidity, and lighting conditions were similar for all groups. Animals had free access to food (regular rat chow) and water delivered through an automated and filtered system. Animals were also handled daily throughout the study so that they could get acclimated to the research personnel thereby decreasing stress. Experiments started one week after arrival of the animals from the breeder and all experimental protocols in this study were approved by the Institutional Animal Care and Use Committee and in accordance with the National Institutes of Health guidelines. We conducted a series of experiments using different rat groups for a total  $n = 52$  (13 rats/group).

### Chemotherapeutic Regimen

Rats in the chemotherapy group received the drug combination of cyclophosphamide (40 mg/Kg; Sigma-Aldrich), methotrexate (37.5 mg/Kg; Wyeth Ayerst, Itasca, IL), and 5-fluorouracil (75 mg/Kg; Sigma-Aldrich) dissolved in normal saline. Rats in the control group received normal saline of equal volume to control for the effects of stress induced by the injection. The dosages selected were based on our preliminary work, which showed that animals tolerated these doses with minimal weight loss or death (Briones and Woods, 2011). Both CMF and normal saline injections were given intraperitoneally once a week for a total of 4 weeks and rats were weighed every other day during the chemotherapeutic regimen. Rats were also monitored daily for other possible toxicity effects of chemotherapy such as apathy, excessive grooming, motor impairment, hair loss, and diarrhea ( $n=2$ ).

### Drug Administration

A cyclooxygenase-2 (COX-2) inhibitor was given to block the inflammatory response. COX-2 is a key synthetase of prostaglandin  $E_2$ , a ubiquitous central proinflammatory mediator, which acts on the brain. We used the selective COX-2 inhibitor, NS-398 (Cayman Chemical, Ann Arbor, MI). The COX-2 inhibitor, NS-398, was dissolved in saline and given at 10 mg/Kg i.p. For the control group, equal volume of saline (vehicle) was injected i.p. Both NS-398 and vehicle were injected one hour after CMF administration and then given daily for 28 days (4 weeks) thereafter.

### Behavioral Testing

Spontaneous object recognition and temporal order memory were tested using the Y maze as previously described (Briones and Darwish, 2012). Rats were habituated to the Y maze without any objects for 1 minute per day for 3 days to reduce anxiety. Tests in the Y maze consisted of: novel object preference, object-in-place, and temporal order memory tasks. Briefly, all tests comprised of an acquisition phase (sample phase) and a recognition phase (test phase), separated by a time delay. The maze and objects were wiped with a wet cloth containing sodium hypochlorite solution after each session to eliminate odor cues. Exploratory behavior was defined as the animal directing its nose or sniffing toward the

object at a distance of ~2 cm. Behaviors such as looking around while sitting on or resting against the object were not considered exploratory behavior.

The *novel object recognition* task allowed discrimination between novel and familiar objects. This kind of memory consisted of two components: recollection, which depends on the hippocampus, and familiarity, which depends on the perirhinal cortex (Barker and Warburton, 2011). The delay between the sample and test phases was 30 minutes. The time spent exploring the novel and familiar objects was recorded for 2 minutes but attention was focused on the first minute, during which rats' preference for the novel object is typically greatest (Mumby et al., 2002). The position of the objects in the test phase and the objects used as novel or familiar were counterbalanced between rats.

The *object-in-place task* was started 2 hours after completion of the novel object recognition test. In this task, the rat's ability to recognize objects it had experienced before that remained in the same location versus those that had changed location was assessed. The delay between the sample and test phases was 60 min and the objects were moved and the positions of the objects were counterbalanced between rats. If object-in-place memory is intact, the animal should spend more time exploring the two objects that are in different locations compared to the two objects that are in the same locations.

*Temporal order memory task* was started 24 hours after completion of the object-in-place test. This task comprised of two sample phases and one test trial. Different objects were used for sample phases 1 and 2, with a delay between the sample phases of 30 min. The test trial (2 min duration) was given 90 minutes after sample phase 2. The positions of the objects in the test and the objects used in sample phases 1 and 2 were counterbalanced between the animals. If temporal order memory is intact, the rats should spend more time exploring the object from sample 1, i.e., the object presented less recently, compared with the object from sample 2, i.e., the new object.

In all the tasks, the rats were placed in the Y maze start box and the guillotine door was opened to allow the rat entry into the main area of the apparatus; the door was closed immediately once the rats had vacated the start box to prevent reentry into this area. Timing of the exploration session did not begin until the rat had exited the start box. The Y shape maze was used to reduce the spatial and contextual information and test only object recognition abilities of the animals. All sessions (acquisition and testing) were recorded using the Ethovision XT<sup>®</sup> v.8.5 video tracking program (Leesburg, VA). The total time exploring each object and the discrimination ratio, which is the difference in time exploring novel and familiar objects divided by the total time were calculated.

## Tissue Preparation

All rats were euthanized using CO<sub>2</sub> asphyxiation after behavioral testing, the brains removed, cut in half sagittally and the corpus callosum was manually dissected then immediately placed in liquid nitrogen and kept frozen until processed. One half was used for immunohistochemistry (oligodendrocyte progenitor cells and myelin basic protein). The other half was used for ELISA and Western blot for determination of cytokines IL-1 $\beta$  and TNF- $\alpha$  protein levels, and COX-2 expression, respectively. A subset of animals (n=5/group) was used to examine myelin structure (myelinated and unmyelinated axons and myelin thickness) and the brains were prepared for electron microscopy. Blinding procedures were employed in all experimental protocols.

### Cytokine Protein Quantification

The concentration of IL-1 $\beta$ , TNF- $\alpha$ , and IL-10 protein levels was determined in the corpus callosum using commercially available ELISA assays, following the instructions supplied by the manufacturer (R&D Systems; Minneapolis, MN). Briefly, 0.2 g of frozen callosal tissue was homogenized with a glass homogenizer in 1 ml buffer containing 1 mmol/liter phenylmethylsulfonyl fluoride, 1 mg/liter pepstatin A, 1 mg/liter aprotinin, and 1 mg/liter leupeptin in PBS (pH 7.2) and centrifuged at 12,000  $\times$  g for 20 minutes at 4°C. The supernatant was collected and total protein was determined by bicinchoninic acid (BCA) protein assay reagent kit (PIERCE, Milwaukee, WI). Samples were used for ELISA to determine IL-1 $\beta$ , TNF- $\alpha$ , and IL-10 protein levels. The procedure was performed according to manufacturer's specification using the Quantikine rat-specific ELISA kits (R&D Systems, Minneapolis, MN) and the color reaction was detected using the chromogen tetramethylbenzidine. Color reaction was stopped by an equal volume of stop solution (provided by the manufacturer) and read in a microplate reader (Bio-Tek, Winooski, VT) at a wavelength of 450 nm (650-nm reference wavelength). The color change was proportional to the concentration of the cytokines measured and all samples measured were within the range of the standard curve. This ELISA system detects both natural and recombinant rat IL-1 $\beta$ , TNF- $\alpha$ , and IL-10. Assays were sensitive to 5 pg/ml for IL-1 $\beta$  and TNF- $\alpha$ , and 10 pg/ml for IL-10; the intra-assay and inter-assay coefficients of variation were <5% and <10% for TNF- $\alpha$  and IL-10, and <6% and <9% for IL-1 $\beta$ . Assays were performed in triplicates and measurements were averaged and used as one individual data point for statistical analysis.

### Western Blot

To detect COX-2 levels 0.5 g of frozen callosal tissue was used in the Western blot procedure. Tissues were homogenized and centrifuged at 25,000  $\times$  g for 20 minutes as previously described (Briones et al., 2006; Briones et al., 2009). Aliquots from the supernatant were removed for protein determination. Protein concentration in samples was determined using the BCA-Protein assay (Pierce, Rockford, IL). Equal amounts of protein (40  $\mu$ g) from each rat were loaded and separated by SDS-PAGE gel electrophoresis in 8% – 16% acrylamide gradient gels. The protein bands were electrophoretically transferred to nitrocellulose membranes (Amersham, Piscataway, NJ) stained with 0.5% Ponceau Red to visualize total proteins, then destained. Non-specific binding sites were blocked then nitrocellulose membranes were incubated overnight at 4°C with gentle agitation in the primary antibody goat anti-COX-2 (1:1000, Santa Cruz Biotechnology, Santa Cruz, CA). The secondary antibodies used were horseradish peroxidase-conjugated immunoglobulin (Sigma, St. Louis, MO) and the Super Signal chemiluminescence substrate kit (Pierce, Rockford, IL) was used to visualize immunoreactive bands. After visualization, the membranes were then stained with Amido-Black to qualitatively verify protein loading. A series of dilutions were performed and immunoblotted for each antibody to establish that the relationship between protein band and intensity was linear over the range of band intensities observed in the samples. Band visualization was obtained by exposure of membranes to autoradiographic film (Kodak Biomax<sup>TM</sup>). Samples were analyzed in quadruplicates and measurements were averaged and used as one individual data point for statistical analysis. Quantification of differences in protein bands between samples was done using densitometric analysis (Scion Image Beta 4.0.2; Frederick MD). The internal control  $\beta$ -actin was used to standardize experimental values in densitometric analysis. Densitometric values were calculated as: density of sample band/density of background.

### Electron Microscopy

Animals were anesthetized with pentobarbital (100 mg/Kg) and transcardially perfused with 100 ml of heparinized 0.1M phosphate buffer (pH 7.3) followed by 50 ml of sodium

cacodylate buffer (pH 7.3) then 400 ml of fixative (2% glutaraldehyde and 2% paraformaldehyde in the same buffer). After perfusion, the whole brain was immediately removed and kept in fixative at 4°C overnight. Following postfixation, a midsagittal cut made, and a 1mm thick slab containing the anterior third of the corpus callosum from the right hemisphere was isolated. The tissue was postfixed with buffered 2% osmium tetroxide, treated en bloc with uranyl acetate, gradually dehydrated in ethanol/propylene oxide, and embedded in an Araldite/Epon resin mixture (Ted Pella, Redding, CA). The blocks were coded to preclude experimenter bias during quantitative morphological analysis. To ensure consistency between groups in procedures that may affect tissue shrinkage and section thickness, tissue from all groups was processed together for each step of histological processing. Semithin sections (1 µm) were taken from the embedded blocks using an ultramicrotome then mounted on gelatin-coated slides and stained with Toluidine blue then coverslipped. An outline of the callosal genu region was traced using a camera lucida (Fig. 1) and the area of the genu was determined using the ImageJ software (v. 1.47).

Using the 1 µm sections as a guide, a pyramid was trimmed from the same block so that only the genu occupy the sectioned area. Ultrathin sections (60–75 nm) were cut from embedded tissue blocks containing the genu using an ultramicrotome and mounted on formvar-coated grids, which were then stained with uranyl acetate and lead citrate and examined using a Philips CM200 transmission electron microscope. Myelinated and unmyelinated axon quantification was performed employing the stereological point counting technique using a grid that has a known number of intersections or points (110 intersection) placed randomly over the digital electron micrographs. The area occupied by the structure of interest (myelinated and unmyelinated axons) was approximated by the number of intersections that falls upon that structure summed over all sampled images (6 images/rat) multiplied by the area of interest (genu region determined from the Toluidine Blue-stained scanned images). In addition, myelin sheath thickness of counted axons were determined using the ImageJ software and myelin thickness measurements were made from portions of individual sheaths without artifactual disruption of lamellae.

### Immunohistochemistry

For immunohistochemistry, the fixed brains (fixative is 4% paraformaldehyde in 0.1M phosphate buffer, pH 7.3) were sectioned at 20 µm thickness using a cryostat. The free-floating sections were first treated with 0.3% hydrogen peroxide in PBS to inactivate endogenous peroxidase activity. After inactivation, the tissues were rinsed and placed in the blocking solution of 3% serum, 0.1% Triton-X, and 1% bovine serum albumin for 1 hour then washed in 0.1M phosphate buffered saline (pH 7.3) followed by incubation for 48 hours at 4°C with antibody recognizing either: 1) oligodendrocyte precursor cells with O4 antigens (monoclonal anti-mouse, 1:1000); or 2) myelin basic protein (monoclonal anti-mouse, 1:1500). The primary antibodies (Chemicon International, Temecula, CA) were detected using biotinylated IgG secondary antibodies (1:400, Vector Laboratories, Burlingame, CA) for 1 hour at room temperature. The tissues were then washed and incubated in avidin-biotin complex (ABC kit, Vector Laboratories, Burlingame, CA) for one hour at room temperature. Immunoreactions were visualized by treatment of tissue sections with hydrogen peroxide and 3,3'-diaminobenzidine tetrahydrochloride (DAB) in Tris buffer (pH 7.3) enhanced with nickel. After thorough rinsing, the tissue sections were mounted on gelatin-coated slides, dried, and coverslipped. Tissues from all experimental groups were run simultaneously and under identical conditions to ensure reproducibility of results. In all immunohistochemical experiments, pre-dilution test were done to ensure specificity of the antibodies and negative controls, involving deletion of the primary antibodies, were used to rule out any nonspecific interactions.

The stereological method of surface density ( $S_v$ ) measurements was used to quantify OPC and myelin immunoreactivity wherein a set of test lines (cycloid arcs) was superimposed on light microscopic images and the intersection between the test lines and immunoreactive cells were counted. Surface density was calculated using the formula:  $S_v = 2(I/L)$ , where  $I$  is the total number of intersections, summed over all samples (6 samples/animal), and  $L$  is the total length of the test line within the sample area (502  $\mu\text{m}$ ).

### Statistical Analysis

The SAS general linear model (SAS Institute, North Carolina) procedures for two-way analysis of variance (ANOVA) were used to examine effects of experimental conditions (CMF vs. saline groups) and COX-2 inhibitor (NS-398 vs. vehicle) on the dependent variables. Two-way repeated measures ANOVA was used to examine CMF and COX-2 inhibitor effects on behavioral performance on the Y maze. When appropriate, the SAS CONTRAST statement was used for planned comparisons. All error bars represented  $\pm$  standard error of the mean (SEM) of the sample size used in the study.

### Results

The main goal of the study was to determine the link between changes in myelination and neuroinflammation as potential mechanisms in chemotherapy-induced cognitive impairment. We examined the effects of CMF-induced neuroinflammation on oligodendrocyte precursor cells (OPCs) and myelin basic protein in the corpus callosum; as well as on myelinated and unmyelinated axons, and myelin sheath thickness in the genu of the corpus callosum. The genu was chosen for electron microscopy analysis because fibers from this area connects the two hemispheres of the prefrontal cortex, brain region involved in working memory (van der Knapp and van der Ham, 2011), which is the most common deficit reported in chemotherapy-related cognitive impairment (Hodgson et al., 2013; Janelins et al., 2011).

#### Chemotherapy induces persistent neuroinflammation

Initially we examined the effects of CMF on the persistent neuroinflammatory response. For this purpose, rats were randomly assigned to either CMF or saline therapy then animals from each group were further randomized to receive either NS-398 (COX-2 inhibitor) or vehicle. After 4 weeks of therapy, rats were allowed to recover for another 4 weeks then tested in the Y maze followed by euthanasia. We examined protein levels of the pro-inflammatory cytokines IL-1 $\beta$  and TNF- $\alpha$  using ELISA and expression of COX-2 using Western blot. Our results indicated significant main effects on IL-1 $\beta$  ( $F(3,48) = 9.88, p < 0.05$ ), TNF- $\alpha$  ( $F(3,48) = 10.06, p < 0.05$ ), and COX-2 ( $F(3,48) = 11.14, p < 0.05$ ) where CMF treatment led to the upregulation of these inflammatory mediators even when therapy was discontinued 4 weeks before euthanasia (Fig. 2A–C). However, giving COX-2 inhibitor immediately after the initial CMF treatment significantly decreased levels of IL-1 $\beta$ , TNF- $\alpha$ , and COX-2 in the corpus callosum to 25%, 39%, and 34%, respectively, when compared to the CMF-treated animals that received vehicle. No significant changes were seen in IL-1 $\beta$ , TNF- $\alpha$ , and COX-2 levels in the saline-treated rats.

In addition, we also examined levels of IL-10 and found significant main effects of CMF ( $F(3,48) = 10.99, p < 0.05$ ) and NS-398 ( $F(3,48) = 11.27, p < 0.05$ ) in IL-10 levels where a downregulation of this anti-inflammatory cytokine was seen 4 weeks after CMF treatment was discontinued. But administration of COX-2 inhibitor immediately after the first dose of CMF treatment significantly modulated the reduction of IL-10 levels. IL-10 levels in the CMF-treated rats that received NS-398 was 36% higher when compared to the CMF-treated animals that received vehicle. No significant differences were seen in IL-10 levels in the

saline-treated rats (Fig. 2D). Together, these results suggest that neuroinflammation occurred in response to CMF and that it can persist even after discontinuation of treatment.

### Chemotherapy induces persistent cognitive impairment

Rats were allowed to recover for 4 weeks after CMF or saline treatment then behavioral testing was performed in the Y maze. Analysis of performance in the *novelty recognition task* showed no significant main effects of CMF and NS-398 in exploration times during the acquisition phase. Separate analysis of exploration times in the test phase also showed no significant group differences as seen in Table 1. Moreover, discrimination ratio on the test phase showed no significant main effect of CMF nor NS-398 wherein all rats demonstrated the ability to discriminate between the familiar and novel objects even after a time delay between the acquisition and test phases (Fig. 3A). Also, no significant interaction effect was seen between CMF and NS-398 in total exploration times and discrimination ratio.

Evaluation of performance in the *object-in-place task* showed no significant group differences in exploration time after a 30 minutes delay (Table 1). But significant main effects of CMF ( $F(3,48) = 10.18, p < 0.05$ ) and NS-398 ( $F(3,48) = 12.30, p < 0.05$ ) were seen in discrimination ratio where the ability to discriminate between the moved object and the object that remained in place was lower in the CMF-treated rats (Fig. 3B). However, this cognitive impairment was mitigated in the CMF-treated animals that received NS-398 even though their discrimination ratio was still less than the saline-treated animals. Comparison of the saline-treated groups showed no significant difference in discrimination ratio in the object-in-place task.

Analysis of recognition in the *temporal order memory test* after a 90-minute delay revealed significant main effects of CMF ( $F(3,48) = 12.11, p < 0.05$ ) and NS-398 ( $F(3,48) = 11.99, p < 0.05$ ) in exploration time as seen in Table 1. Post hoc testing confirmed that exploration time of the CMF-treated rats that received vehicle was significantly worse when compared to all groups (Table 1). But CMF-treated rats given NS-398 showed improvement in exploration time when compared to the CMF-treated group that received vehicle even though their performance is still impaired in comparison to the saline treated groups. No significant difference was seen in exploration time between the saline-treated groups. Analysis of discrimination ratio also showed significant main effects of CMF ( $F(3,48) = 12.11, p < 0.05$ ) and NS-398 ( $F(3,48) = 11.80, p < 0.05$ ) where CMF-treatment resulted in decrease ability able to discriminate between the objects presented earlier and the one presented recently. However, post hoc comparison showed that CMF-treated rats that received NS-398 performed  $\approx 80\%$  better than the CMF group that received vehicle. But administration of NS-398 to the CMF group did not completely eliminate the cognitive deficit in the temporal order memory task when compared to the saline-treated rats. Together, these results suggest that cognitive impairment persisted even after discontinuation of treatment and that modulating the inflammatory response may be able to ameliorate CMF-related cognitive impairment.

### Chemotherapy induces myelination and myelin abnormalities

Next we aimed at evaluating the involvement of chemotherapy and neuroinflammation on structural changes in myelin and myelination. Our results showed a significant main effect of CMF ( $F(3,48) = 10.43, p < 0.05$ ) and NS-398 ( $F(3,48) = 11.01, p < 0.05$ ) in O4 immunoreactivity. As well, a significant main effect of CMF ( $F(3,48) = 12.08, p < 0.05$ ) and NS-398 ( $F(3,48) = 10.91, p < 0.05$ ) was seen in myelin basic protein immunoreactivity (Fig. 4). Significant decreased in O4 and myelin basic protein (MBP) immunoreactivities were seen after CMF treatment; but post hoc comparisons showed that administration of NS-398 significantly attenuated the reduction in O4 and MBP immunoreactivities induced by CMF.



Yet NS-398 administration did not completely stop the CMF-induced loss in O4 and MBP immunoreactivities. No significant differences in O4 and MBP immunoreactivities were seen in the saline-treated groups.

When we examined the myelin structure, we found a significant main effect of CMF and NS-398 in the area of the genu covered by myelinated axons. Additionally, a significant main effect of CMF ( $F(3,48) = 11.05, p < 0.05$ ) and NS-398 ( $F(3,48) = 10.78, p < 0.05$ ) was seen in the area of the genu covered by unmyelinated axons. CMF treatment resulted in decreased area of the genu covered by myelinated axons while the area covered by unmyelinated axons increased suggesting myelin loss. But then posthoc comparisons showed that administration of NS-398 to CMF-treated rats significantly reduced the chemotherapy-induced myelin loss; although the area occupied by myelinated and unmyelinated axons in the CMF-treated rats that received NS-398 was still significantly decreased in relation to the saline-treated animals.

Quantification of the thickness of myelin sheath in the genu region of the corpus callosum also showed significant main effects of CMF ( $F(3,48) = 10.14, p < 0.05$ ) and NS-398 ( $F(3,48) = 10.32, p < 0.05$ ). Overall, myelin sheath thickness was significantly less in the CMF rats given vehicle but posthoc comparisons showed that giving NS-398 to CMF-treated rats during and after treatment significantly attenuated the decrease in myelin sheath thickness. However, myelin sheath thickness in the CMF-treated rats given NS-398 still showed significantly less thickness in their myelin sheath thickness when compared to the saline-treated groups. No significant differences were seen in myelin sheath thickness in the saline-treated groups. Together, these results suggest the involvement of neuroinflammation in CMF-induced effects on myelination and myelin structure.

## Discussion

In the present study we show that CMF therapy results in persistent neuroinflammation, and that neuroinflammation is involved in CMF-induced cognitive dysfunction and changes in myelin structure and myelination. These findings are supported by our data that: (1) CMF therapy led to the increase in levels of inflammatory mediators IL-1 $\beta$ , TNF- $\alpha$ , and COX-2 while levels of the anti-inflammatory cytokine IL-10 decreased; (2) both cognitive impairment and neuroinflammation resulting from CMF therapy persisted 4 weeks after the treatment ended; and (3) administration of the COX-2 inhibitor, NS-398, attenuated CMF-induced neuroinflammation, effects on myelination, and cognitive impairment. Ultimately, these findings suggest the intricate involvement of neuroinflammation in CMF-induced structural effects in the corpus callosum and cognitive impairment; and to our knowledge this is the first study to address this area of investigation.

Neuroinflammation is an important compensatory mechanism of the brain when it encounters an insult where an upregulation of inflammatory mediators are triggered (Block and Hong, 2005). As a compensatory mechanism following an insult, neuroinflammation has clear beneficial effects only if it is controlled in a regulated manner and for a defined period of time (Finnie, 2013). However, if the neuroinflammatory process persists it can contribute to neurodegeneration and neurological impairments (Lucin and Wyss-Coray, 2009). Our data on upregulation of the inflammatory mediators IL-1 $\beta$ , TNF- $\alpha$ , and COX-2 together with down regulation of the anti-inflammatory cytokine IL-10 weeks after discontinuation of CMF treatment suggest the persistent nature of neuroinflammation induced by the cytotoxic effects of chemotherapy. These results are in contrast with a previous study that reported decrease plasma cytokine expression while no increase in central cytokine levels seen following methotrexate treatment in rats (Seigers et al., 2010b). A possible explanation for the contrasting findings is that our study used the combination

treatment of cyclophosphamide, methotrexate, and 5-fluorouracil while the other study used methotrexate alone. Therefore, it is possible that the addition of cyclophosphamide and 5-fluorouracil increased the cytotoxicity levels of the chemotherapeutic regimen used in the present study since an earlier report show that 5-fluorouracil alone can cause damage to oligodendrocytes (Dietrich et al., 2006; Han et al., 2008). Furthermore, decreased levels of pro-inflammatory cytokines reported in the other study are in conflict with our data on increased IL-1 $\beta$  and TNF- $\alpha$ . This difference may be explained by the fact that we measured central expression of pro-inflammatory cytokines in the corpus callosum while the other study measured plasma levels. It is highly likely that cytokine expression in the brain will differ from peripheral expression in plasma.

The vulnerability of both cerebral white and gray matters to the cytotoxic effects of chemotherapy have been well document in neuroimaging studies [reviewed in (Simo et al., 2013)]. For example, reports show late effects (10 years) of high-dose adjuvant chemotherapy on white matter structure (decreased fractional anisotropy and increased diffusivity) in breast cancer survivors (de Ruitner et al., 2011). Others also report decreased white matter tracts in cancer survivors given standard-dose chemotherapy from months to years after treatment (Abraham et al., 2008; Deprez et al., 2011). White matter is composed of myelinated axons and oligodendrocytes. The O4 cells examined in the present study are pre-myelinating precursor cells formed postnatally (Schachner et al., 1981) and is a marker for cell bodies and processes of oligodendrocytes types I and II. During oligodendrocyte differentiation, O4 occurs in pro-oligodendrocytes, but not in O-2A-progenitor cells, thus it is commonly used in myelination, demyelination and remyelination studies. MBP on the other hand is a major structural protein of myelin sheaths (Baumann and Pham-Dinh, 2001). In the present study, we examined the corpus callosum because it is the largest white matter structure in the brain and is primarily comprised of both myelinated and unmyelinated axons. Myelin structures are formed by oligodendrocytes and our data suggest the possibility of chemotherapy-induced impairment in myelin formation. This logic is reflected on our results on decreased O4 immunoreactivity and validated by a previous study showing the cytotoxic effects of 5-Fluorouracil on oligodendrocytes (Dietrich et al., 2006; Han et al., 2008). Our results showing decreased MBP immunoreactivity provide further support on the vulnerability of white matter structures to the cytotoxic effects of chemotherapy since this protein directly correlates with levels of myelination (Campagnoni and Maeklin, 1988). Our findings are also in line with a previous report on delayed white matter degeneration in rats after treatment with 5-Fluorouracil (Han et al., 2008). The persistent neuroinflammation seen in our study most likely explain CMF-induced changes in myelination and myelin structure. What is not clear from the present study is whether the neuroinflammation and myelination changes seen after 4 weeks of chemotherapy is a delayed effect or an acute response that persisted during the recovery period. This issue warrants further investigation in future studies.

Our data on decreased area occupied by myelinated axons while area occupied by unmyelinated axons increased associated with CMF treatment are also not surprising. These findings together with the decreased thickness in myelin sheaths seen in the CMF-treated rats may be explained by the reduction in MBP levels. MBP constitutes 25% of the myelin in the central nervous system and has been documented to be involved in the myelination process and the compaction of myelin sheath. Interestingly, blocking the neuroinflammatory response to CMF treatment offset the detrimental effects of chemotherapy on myelin and the myelination suggesting a direct link between CMF-induced neuroinflammation and myelin breakdown.

The present study also reinforces previous reports on the relationship between myelin structure changes and cognitive impairment. Our data show that CMF-induced decrease in

OPCs and MBP immunoreactivities as well as reduction in myelinated axons and myelin sheath thickness are associated with cognitive impairment. The findings in the present study are in line with neuroimaging studies that show decreased white matter densities in the prefrontal cortex correlates with decreased reaction time (Gold et al., 2010), information processing speed (Lu et al., 2011; Lu et al., 2013), and executive functioning involving attentional set-shifting and working memory [(Kennedy and Rax, 2009) also reviewed in (Simo et al., 2013)]. More importantly, the imaging study results are consistent whether done in normal aged subjects or cancer survivor patients that received chemotherapy.

A surprising finding in the present study is the fact that administration of COX-2 inhibitor did not completely abolish the effects of CMF on myelination and cognitive function. A possible reason for these unexpected findings is that cyclooxygenases derived from prostaglandin exist in two isoforms COX-1 and COX-2 (Pepicelli et al., 2005). These two isoforms share 60% homology but may play different roles in neuroinflammation (Phillis et al., 2006). Traditionally, COX-2 is recognized as the enzyme produced resulting from an inflammatory event even though both isoforms are constitutively expressed in the brain. But recent reports show that COX-1 also plays a role in neuroinflammation due to its predominant location in microglial cells [reviewed in (Aid and Bosetti, 2011)]. Thus, it is possible that by blocking only COX-2 our results show only partial inhibition of the neuroinflammatory response.

Another reason is that recent reports show that COX-2 may also have an anti-inflammatory response (Yang and Chen, 2008). For example, some studies show that COX-2 deletion increased neuronal damage, glial activation, and the expression of the inflammatory cytokine IL-1 $\beta$  as well as free radicals (Aid and Bosetti, 2011). Therefore, it is possible that by administering COX-2 inhibitor to the CMF rats in the present study we extinguished the protective effects of COX-2 and instead aggravated the cytotoxic effects of chemotherapy. However, this seems improbable given that use of COX-2 inhibitor during and after CMF therapy in the present study modulated the neuroinflammatory response and the toxic effects of chemotherapy on myelination and cognitive function.

In sum, our study shows proof of concept that neuroinflammation is involved in CMF-induced cognitive impairment and effects on myelination. The association between myelination changes in the corpus callosum and CMF-induced may have be mediated by the persistent neuroinflammation induced by the cytotoxic effects of chemotherapy. Because CMF-induced cognitive impairment was not completely abolished by administration of COX-2 inhibitor in our study, it also raises the possibility that neuroinflammation may not be the only biochemical process triggered by CMF that can affect myelination and cognition. Future studies on the role of key growth factors and cellular signaling mechanisms on CMF-induced cognitive impairment can address this issue.

## Acknowledgments

This work was supported in part by the National Institutes of Health, NINR grant # RO1 NR007666 and the Wayne State University Katharine Faville Endowment Funds. We are grateful for the assistance of Maggie Wadowska in animal handling and Maria Palu in tissue imaging.

## References

- Abraham J, et al. Adjuvant chemotherapy for breast cancer: effects on cerebral white matter seen in diffusion tensor imaging. *Clin Breast Cancer*. 2008; 8:88–91. [PubMed: 18501063]
- Ahles TA, Saykin AJ. Breast cancer chemotherapy-related cognitive dysfunction. *Clin Breast Cancer*. 2002; 3:S84–S90. [PubMed: 12533268]

- Aid S, Bosetti F. Targeting cyclooxygenases-1 and -2 in neuroinflammation: therapeutic implications. *Biochimie*. 2011; 93:46–51. [PubMed: 20868723]
- Barker GRI, Warburton EC. When is the hippocampus involved in recognition memory? *J Neurosci*. 2011; 31:10721–10731. [PubMed: 21775615]
- Baumann N, Pham-Dinh D. Biology of oligodendrocyte and myelin in the mammalian central nervous system. *Physiol Rev*. 2001; 81:871–927. [PubMed: 11274346]
- Block ML, Hong JS. Microglia and inflammation-mediated neurodegeneration: multiple triggers with a common mechanism. *Prog Neurobiol*. 2005; 76:77–98. [PubMed: 16081203]
- Boykoff N, Moieni M, Subramanian SK. Confronting chemobrain: an in-depth look at survivors' reports of impact on work, social networks, and health care response. *J Cancer Survivor*. 2009; 3:223–232.
- Briones TL, et al. Amelioration of cognitive impairment and changes in microtubule-associated protein 2 after transient global cerebral ischemia are influenced by complex environment experience. *Behav Brain Res*. 2006; 168:261–271. [PubMed: 16356557]
- Briones TL, Rogozinska M, Woods J. Environmental experience modulates ischemia-induced amyloidogenesis and enhances functional recovery. *J Neurotrauma*. 2009; 24:613–625. [PubMed: 19271963]
- Briones TL, Rogozinska M, Woods J. Modulation of ischemia-induced NMDAR1 activation by environmental enrichment decreases oxidative damage. *J Neurotrauma*. 2011; 28:2485–2492. [PubMed: 21612313]
- Briones TL, Woods J. Chemotherapy-induced cognitive impairment is associated with decreases in cell proliferation and histone modifications. *BMC Neurosci*. 2011; 9:124. [PubMed: 22152030]
- Briones TL, Darwish H. Vitamin D mitigates age-related cognitive decline through the modulation of pro-inflammatory state and decrease in amyloid burden. *J Neuroinflammation*. 2012; 9:244. [PubMed: 23098125]
- Campagnoni AT, Maeklin WB. Cellular and molecular aspects of myelin basic protein gene expression. *Mol Neurobiol*. 1988; 2:41–89. [PubMed: 3077065]
- Castellon SA, Ganz PA. Neuropsychological studies in breast cancer: in search of chemobrain. *Breast Cancer Res Treat*. 2009; 116:125–127. [PubMed: 18923899]
- Correa DD, Ahles TA. Cognitive adverse effects of chemotherapy in breast cancer patients. *Curr Opin Support Palliat Care*. 2007; 1:57–62. [PubMed: 18660726]
- de Ruitner MB, et al. Cerebral hyporesponsiveness and cognitive impairment 10 years after chemotherapy for breast cancer. *Hum Brain Mapp*. 2011; 32:1206–1219. [PubMed: 20669165]
- Deprez S, et al. Chemotherapy-induced structural changes in cerebral white matter and its correlation with impaired cognitive functioning in breast cancer patients. *Hum Brain Mapp*. 2011; 32:480–493. [PubMed: 20725909]
- Dietrich J, et al. CNS progenitor cells and oligodendrocytes are targets of chemotherapeutic agents in vitro and in vivo. *J Biol*. 2006; 5:22.1–22.23. [PubMed: 17125495]
- Finnie JW. Neuroinflammation: beneficial and detrimental effects after traumatic brain injury. *Inflammopharmacology*. 2013
- Gold BT, et al. Age-related slowing of task switching is associated with decreased integrity of frontoparietal white matter. *Neurobiol Aging*. 2010; 31:512–522. [PubMed: 18495298]
- Han R, et al. Systemic 5-fluorouracil treatment causes a syndrome of delayed myelin destruction in the central nervous system. *J Biol*. 2008; 7:12. [PubMed: 18430259]
- Hodgson KD, et al. A meta-analysis of the effects of chemotherapy on cognition in patients with cancer. *Cancer Treat Rev*. 2013; 39:297–304. [PubMed: 23219452]
- Inagaki M, et al. Smaller regional volumes of brain gray and white matter demonstrated in breast cancer survivors exposed to adjuvant chemotherapy. *Cancer*. 2007; 109:146–156. [PubMed: 17131349]
- Janelins MC, et al. Cognitive difficulties, fatigue, and sleep in cancer patients at pre-chemotherapy, post-chemotherapy, and at three months follow-up. *Ann Behav Med*. 2010:39.
- Janelins MC, et al. An update on cancer- and chemotherapy-related cognitive dysfunction: current status. *Semin Oncol*. 2011; 38:431–438. [PubMed: 21600374]

- Kennedy KM, Rax N. Aging white matter and cognition: differential effects of regional variations in diffusion properties on memory, executive functions, and speed. *Neuropsychologia*. 2009; 47:916–927. [PubMed: 19166865]
- Kesler SR, et al. Regional brain activation during verbal declarative memory in metastatic breast cancer. *Clin Cancer Res*. 2009; 15:6665–6673. [PubMed: 19843664]
- Koppelmans V, et al. Incidental findings on brain Magnetic Resonance Imaging in long-term survivors of breast cancer treated with adjuvant chemotherapy. *Eur J Cancer*. 2011;10.1016/j.ejca.2011.06.026
- Koppelmans V, et al. Global and focal white matter integrity in breast cancer survivors 20 years after adjuvant chemotherapy. *Hum Brain Mapp*. 2012:1–11.
- Lu PH, et al. Age-related slowing in cognitive processing speed is associated with myelin integrity in a very healthy elderly sample. *J Clin Exp Neuropsychol*. 2011; 33:1059–1068. [PubMed: 22133139]
- Lu PH, et al. Myelin breakdown mediates age-related slowing in cognitive processing speed. *Brain Cogn*. 2013; 81:131–138. [PubMed: 23195704]
- Lucin KM, Wyss-Coray T. Immune activation in brain aging and neurodegeneration: too much or too little? *Neuron*. 2009; 64:110–122. [PubMed: 19840553]
- McDonald BC, et al. Gray matter reduction associated with systemic chemotherapy for breast cancer: a prospective MRI study. *Breast Cancer Res Treat*. 2010; 123:819–828. [PubMed: 20690040]
- Mumby DG, et al. Hippocampal damage and exploratory preferences in rats: memory for objects, places, and context. *Learn Mem*. 2002; 9:49–57. [PubMed: 11992015]
- Nelson CJ, Nandy N, Roth AJ. Chemotherapy and cognitive deficits: mechanisms, findings, and potential interventions. *Palliat Support Care*. 2007; 5:273–280. [PubMed: 17969831]
- Pepicelli O, et al. Cyclo-oxygenase-1 and -2 differently contribute to prostaglandin E2 synthesis and lipid peroxidation after *in vivo* activation of *N*-methyl-D-aspartate receptors in rat hippocampus. *J Neurochem*. 2005; 93:1561–1567. [PubMed: 15935072]
- Phillis JW, Horrocks LA, Farooqui AA. Cyclooxygenases, lipoxygenases, and epoxygenases in CNS: their role and involvement in neurological disorders. *Brain Res Rev*. 2006; 52:201–243. [PubMed: 16647138]
- Reid-Arndt SA. Breast cancer and “chemobrain”: the consequences of cognitive difficulties following chemotherapy and potential for recovery. *Mol Med*. 2009; 106:127–131.
- Sakane T, et al. Transnasal delivery of 5-fluorouracil to the brain in the rat. *J Drug Target*. 1999; 7:233–240. [PubMed: 10680979]
- Schachner M, Kim SK, Zehnle R. Developmental expression in central and peripheral nervous system of oligodendrocyte cell surface antigens (O antigens) recognized by monoclonal antibodies. *Dev Biol*. 1981; 83:328–338. [PubMed: 6786943]
- Seigers R, et al. Long-lasting suppression of hippocampal cell proliferation and impaired cognitive performance by methotrexate in the rat. *Behav Brain Res*. 2008; 186:168–175. [PubMed: 17854921]
- Seigers R, et al. Inhibition of hippocampal cell proliferation by methotrexate in rats is not potentiated by the presence of a tumor. *Brain Res Bull*. 2010a; 81:472–476. [PubMed: 19828128]
- Seigers R, et al. Methotrexate reduces hippocampal blood vessel density and activates microglia in rats but does not elevate central cytokine release. *Behav Brain Res*. 2010b; 207:265–272. [PubMed: 19840821]
- Silverman DH, et al. Altered frontocortical, cerebellar, and basal ganglia activity in adjuvant-treated breast cancer survivors 5–10 years after chemotherapy. *Breast Cancer Res Treat*. 2007; 103:303–311. [PubMed: 17009108]
- Simo M, et al. Chemobrain: a systematic review of structural and functional neuroimaging studies. *Beurosci Biobehav Rev*. 2013; 37:1311–1321.
- van der Knapp LJ, van der Ham IJM. How does the corpus callosum mediate interhemispheric transfer? a review. *Behav Brain Res*. 2011; 223:211–221. [PubMed: 21530590]
- Weiss B. Chemobrain: a translational challenge for neurotoxicology. *Neurotoxicology*. 2008; 29:891–898. [PubMed: 18479752]

- Woodcock T, Morganti-Kossmann MC. The role of markers of inflammation in traumatic brain injury. *Front Neurol.* 2013; 4:18. [PubMed: 23459929]
- Yang H, Chen C. Cyclooxygenase-2 in synaptic signaling. *Curr Pharm Des.* 2008; 14:1443–1451. [PubMed: 18537667]

**Highlight**

Our study shows proof of concept that myelin changes mediated by neuroinflammation is a possible mechanism in chemotherapy-induced cognitive deficit.



**Figure 1. Camera Lucida drawing of the corpus callosum**  
The region sampled in the study for electron microscopy was the genu.



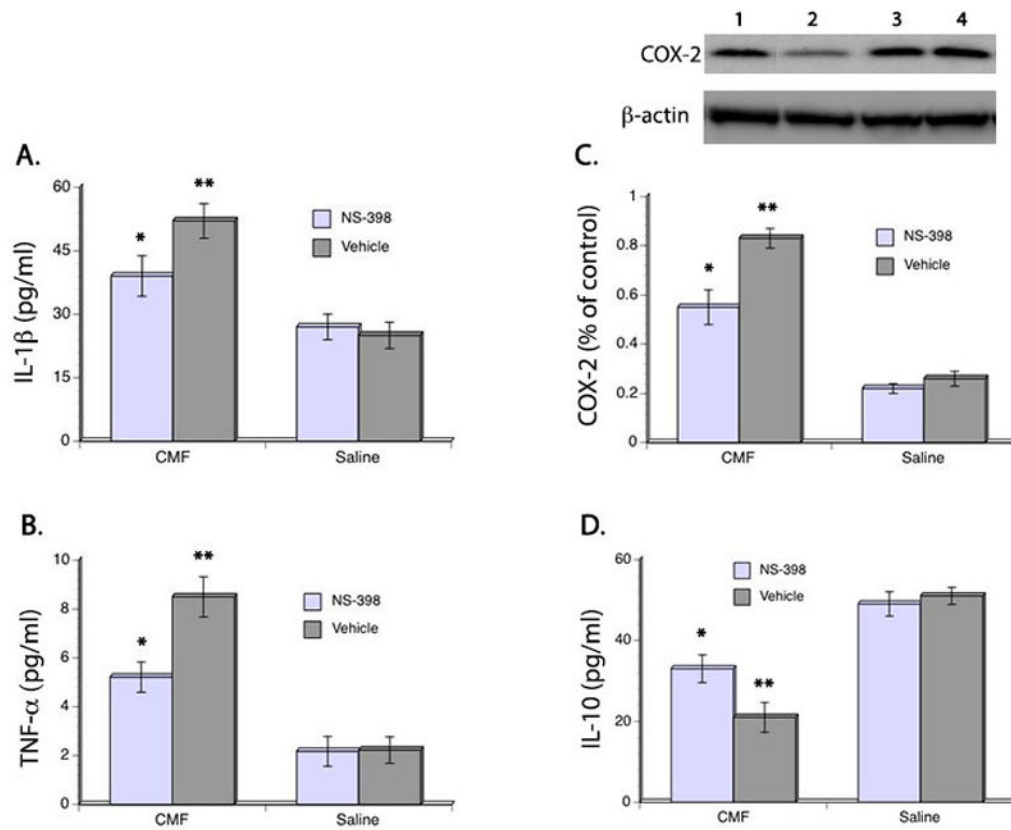


**Figure 2. Expression of Inflammatory markers in the Corpus Callosum**

ELISA showed significant increase in IL-1 $\beta$  (A), TNF- $\alpha$  (B), and COX-2 (C) after CMF treatment but administration of COX-2 inhibitors lessened the upregulation of these inflammatory mediators. ELISA also showed that CMF treatment resulted in decrease levels of the anti-inflammatory cytokine IL-10. No significant differences were seen in the saline-treated groups. Representative Western blot is shown on the upper panel (C). Legends: 1 = CMF/NS-398; 2 = CMF/vehicle; 3 = Saline/NS-398; 4 = Saline/vehicle. \* $p < 0.05$ , \*\* $p < 0.01$ .

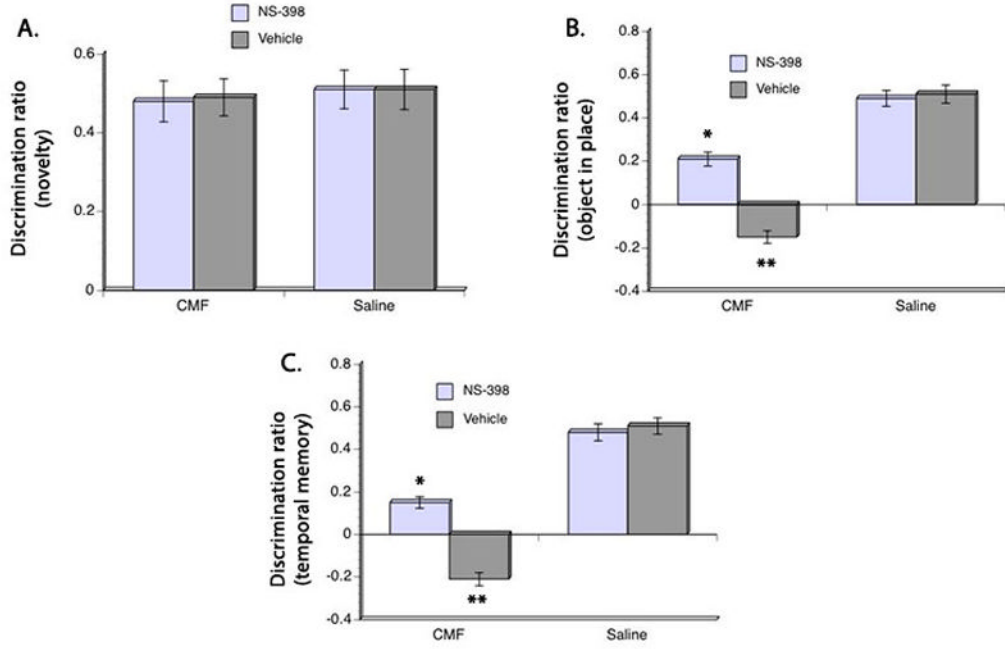


**Figure 3. Behavioral performance in the Y maze**

Discrimination ratio in the novelty object test (A) showed no significant differences in all groups. However, CMF rats showed significant impairment in discriminating between the objects presented in the object-in-place test (B) and temporal order memory test (C) compared to the saline group but administration of NS-398 ameliorated the CMF-induced cognitive impairment. However, performance of the CMF-treated rats given NS-398 is still impaired in the object-in-place and temporal order memory task when compared to the saline group. No significant differences were seen in the performance of the saline groups. \*p <0.05, \*\*p <0.01.

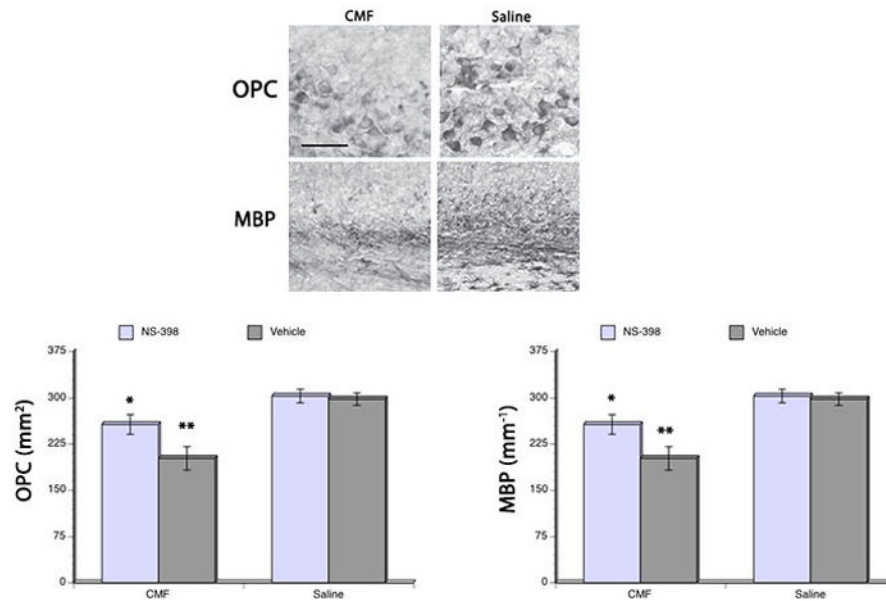


**Figure 4. O4 pre-myelinating cells and myelin basic protein (MBP) expression**  
 CMF treatment resulted in decrease O4 (lower left) and MBP (lower right) immunoreactivities in the corpus callosum, but administration of NS-398 diminished the cytotoxic effects of the chemotherapy on O4 and MBP. However, CMF-treated rats that received NS-398 still showed a reduction in both OPCs and MBP compared to the saline-treated rats. Representative photomicrographs of O4 and MBP immunoreactions in the corpus callosum (upper panel). \* $p < 0.05$ , \*\* $p < 0.01$ . Scale bar = 20  $\mu\text{m}$ .

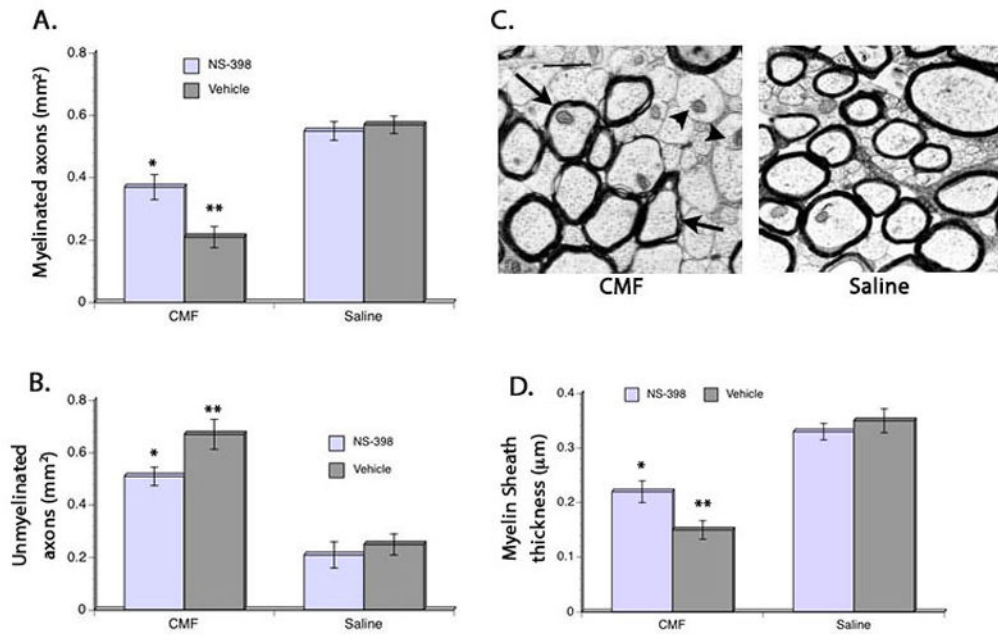


**Figure 5. Axon myelination and thickness**

CMF treatment resulted in decrease area occupied by myelinated axons (A) and increased area occupied by unmyelinated axons (B) in the genu region of the corpus callosum, but administration of NS-398 diminished the cytotoxic effects of the chemotherapy on myelination. However, CMF-treated rats that received NS-398 still show decreased myelinated axons and increased unmyelinated axons compared to the saline-treated rats. No significant groups differences were seen in the saline-treated animals. Similar pattern of CMF and NS-398 effects were seen when myelin thickness was measured (D). Representative digital electron micrographs (C) showing myelinated axons (arrows) and unmyelinated axons (arrowhead). \* $p < 0.05$ , \*\* $p < 0.01$ . Scale bar = 1  $\mu\text{m}$ .

**Table 1**  
**Exploration time in the Y maze**

Mean exploration time expressed in seconds during the sample and test phases in the novelty recognition test, and during the test phases in the object-in-place and temporal order memory tests. No significant differences were seen in exploration time during the novelty recognition task. Meanwhile, CMF-treated rats showed significantly decrease exploration time in the object-in-place and temporal order memory tests after a time delay overall. Although performance improvement was seen in the CMF-treated rats given NS-398, they still showed significantly decrease exploration time when compared to the saline-treated animals.

	<u>Novel Object preference</u>		<u>Object-in-place</u>	<u>Temporal Order Memory</u>
	<b>Sample Phase (s)</b>	<b>Test Phase (s)</b>	<b>Test Phase (s)</b>	<b>Test Phase (s)</b>
CMF/NS-398	42.7 ± 2.71	44.1 ± 2.91	21.5 ± 3.47*	23.3 ± 2.60*
CMF/vehicle	44.2 ± 2.13	47.3 ± 2.83	14.2 ± 2.72**	13.1 ± 2.41**
Saline/NS-398	45.8 ± 1.99	46.2 ± 3.01	31.7 ± 2.14	30.1 ± 2.26
Saline/vehicle	47.3 ± 1.87	46.5 ± 2.72	29.9 ± 2.40	31.9 ± 2.11

No significant differences were seen in the saline groups.

\*  
p <0.05,

\*\*  
p <0.01.